

## A Theoretical Study of the Dynamical Behavior of SQW GaAs/AlGaAs Laser

Dr. Azhar I. Hassan\*

Received on: 15/4/2009

Accepted on: 2/9/2010

### Abstract

In this work, the peak modal gain and the radiative and Nonradiative current densities for Single Quantum Well (SQW) GaAs/AlGaAs laser are studied theoretically with varying the well widths  $L_z=(200, 150, 100, \text{ and } 75) \text{ \AA}$ , at a bandgap discontinuity  $\Delta E_c$  of 0.1 eV, it was found that the highest value of the peak modal gain  $g_{\max}=400 \text{ cm}^{-1}$  is achieved at  $L_z=75 \text{ \AA}$ , and the lower value to achieve transparency  $N_{tr}=0.5 \times 10^{18} \text{ cm}^{-3}$  at  $L_z=200 \text{ \AA}$ .

The optimum value for QW width to achieve the lower threshold current density  $J_{th}=481.5 \text{ A/cm}^2$  at the same injected carrier density is  $L_z=100 \text{ \AA}$ .

**Keywords:** SQW GaAs/AlGaAs laser, Peak gain, Threshold current density.

### دراسة نظرية للسلوك الديناميكي للبئر الكمي الاحادي لليزر GaAs/AlGaAs الخلاصة

جرى في هذا البحث دراسة نظرية لشكل قمة الكسب وكثافات التيارات الاشعاعية والاشعاعية لليزر احادي البئر الكمي نوع GaAs / AlGaAs مع تغير عرض الجدار  $L_z=(200, 150, 100, \text{ and } 75) \text{ \AA}$  عند فجوة طاقة غير مستمرة  $\Delta E_c = 0.1 \text{ eV}$  وقد وجد ان اعلى قيمة لقمة الكسب في الموديل  $g_{\max}=400 \text{ cm}^{-1}$  عند عرض جدار  $L_z=75 \text{ \AA}$  و اقل قيمة للحصول على شفافية  $N_{tr}=0.5 \times 10^{18} \text{ cm}^{-3}$  عند عرض جدار  $L_z=200 \text{ \AA}$ . كانت افضل قيمة لعرض البئر الكمي هي  $L_z=100 \text{ \AA}$  للحصول على اقل عتبة كثافة تيار  $J_{th}=481.5 \text{ A/cm}^2$  عند نفس كثافة الحاملات المحقونة.

### Introduction

Quantum-well (QW) semiconductor lasers offer the advantages of low threshold current density and high-power capability with good efficiency, [1]. Quantum well (QW) lasers are attractive for research because they are both physically very interesting and technologically important. QW technology allows the crystal grower for the first time to control the range, depth, and the arrangement of the quantum mechanical potential wells. In the last decade, the importance of the quantum well laser has steadily grown until today it is preferred for

most semiconductor laser applications, [2,3].

Their growing popularity is because, in almost every respect, the quantum well laser is somewhat better than conventional lasers with bulk active layers. One obvious advantage is the ability to vary the lasing wavelength merely by changing the width of the quantum of the QW. A more fundamental advantage is that the QW lasers delivers more gain per injected carrier than conventional lasers, which results in lower threshold currents, [2,4].

A principal feature of the QW laser is the extremely high

\* Applied Sciences Department, University of Technology/Baghdad

optical gain that can be obtained in the QW for low current densities. This arises partly from greater population inversion at a given carrier density because of the lower quantized density of states, but mostly from the high carrier density in the QW because of its small width, [1,5].

In general, the QW lasers have the extremely high optical gain because of their high carrier confinement. The optical confinement factor of the QW lasers is relatively low due to their thin active region. To predict the lasing behavior, we must evaluate the modal gain of the QW lasers. The modal gain of QW lasers is determined by their optical confinement factor and their ability to collect injected carriers efficiently, [6,7].

In this paper, the primary goal is to study the peak modal gain and the radiative and Nonradiative current densities for Single Quantum-well SQW GaAs/AlGaAs laser theoretically by using matlab language (version 7.4) with varying the well widths  $L_z$  at a bandgap discontinuity of  $\Delta E_c$  of 0.1 eV, and then finding the optimum value for QW width to achieve the lower threshold current density  $J_h$ .

**Theoretical Background:**

The present model calculates the laser gain on the basis of band-to-band transitions, the following assumptions are used in this model:

1. the wells in the conduction and valence bands are approximated by infinitely deep square wells,
2. the bandgap discontinuity is ( $\Delta E_c/\Delta E_v=0.67/0.33$ ),
3. transitions to light and heavy hole subbands,
4. transitions from subbands with the same quantum numbers.

For each quantized level, there is a continuum of energies arising from the lateral kinetic energy of the carriers in the plane of the QW. Associated with each discrete level, the resulting sheet density of states for energies above the minimum level is,[2]

$$r_{QW}(E) = \sum_{n=1}^{all\ states} \frac{m_c}{\pi \hbar^2} H(E - E_{nc}) \dots (1)$$

where:

$E_n$ : is the energy of subband n,

$m_c$ : is the effective mass of the electron at the bottom of the conduction band.

Since  $\rho_{QW}$  is constant in each subband, the density of electrons  $N_e$  and holes  $N_h$  can be calculated analytically and the result will be, [4]:

$$N_e = kT \sum_n \left( \frac{m_c}{\pi \hbar^2 L_z} \right) \ln \left[ 1 + \exp \left( \frac{E_{Fc} - E_{nc}}{kT} \right) \right] \dots (2)$$

$$N_h = kT \sum_n \left( \frac{m_v}{\pi \hbar^2 L_z} \right) \ln \left[ 1 + \exp \left( \frac{E_{Fv} + E_{nv}}{kT} \right) \right] \dots (3)$$

where:

$E_F$  is Fermi energy,

$L_z$  is the layer thickness, of the QW,

$m_v$  is the effective mass of the electron at the top of the valence band.

Under steady-state conditions the rate at which carriers are injected into the active region must equal the electron-hole recombination rate, [4]:

$$\frac{J}{q} = \frac{NL_z}{t} \dots (4)$$

where:

J : is the injected carrier density,

q: is the charge of the electron,

$\tau$  :is the electron-hole recombination time.

The optical gain is calculated using standard perturbation theory Fermi's Golden Rule, (neglecting the effect of intraband scattering). Since the gain anisotropy favors lasing in TE modes, we calculate the gain only for this polarization. The spectrally dependent gain coefficient for the quantum well region is, [8]:

$$g(E) = \frac{q^2 |M|^2}{E e_o m^2 c_o \hbar L_z} * \sum_{i,j} m_r C_{ij} A_{ij} [f_c - (1 - f_v)] H(E - E_{ij}) \quad \dots(5)$$

where:

$|M|^2$ =bulk momentum transition matrix element,

$e_o$ =free-space permittivity,

$m$ =free electron mass,

$c_o$ =vacuum speed of light,

$N$ =effective refractive index,

$i,j$ = conduction, valence quantum numbers (at  $\Gamma$ ),

$m_r$ =spatially weighted reduced mass,

$C_{ij}$ = spatial overlap factor between states  $i$  and  $j$ ,

$A_{ij}$ =anisotropy factor for transition  $i, j$ ,

$f_c$ =Fermi population factor for conduction electrons,

$f_v$ =Fermi population factor for valence holes,

$H$ = Heaviside step function,

$E_{ij}$ =transition energy between states  $i$  and  $j$ .

The bulk averaged momentum matrix element between conduction and valence states is, [9]:

$$|M|^2 = \frac{m^2 E_g (E_g + \Delta)}{6m_c (E_g + 2\Delta/3)} \quad \dots(6)$$

where:

$$E_g = \left[ E_o - \frac{5.405 \times 10^{-4} \times T^2}{T + 204} \right], \quad \dots(7)$$

$E_g$  = direct bandgap,

$E_o$  = bandgap constant,

$T$  = operating temperature,

$\Delta s-o$  = split-off band separation,

The radiative component of carrier recombination is found from the spectrally dependent spontaneous emission rate, [1]:

$$R(E) = \frac{16 p^2 N q^2 E |M|^2}{e_o m^2 c_o^3 h^4 L_z} * \sum_{i,j} m_r C_{ij} [f_c \cdot f_v] H(E - E_{ij}) \quad \dots(8)$$

Equation (8) is an expression for the total spontaneous emission density into all angles and at all polarizations, and therefore does not contain the polarization anisotropy, which has removed by angular integration.

The radiative QW component of the current is calculated from the integral over the spontaneous emission spectrum of the QW, is given by, [2]:

$$J_r = L_z q \int_{E_{g,h1}}^{E_{g,b}} R_{sp}(E) dE \quad \dots(9)$$

where:

$E_{g,h1}$  = transitions at the lower cutoff at the effective bandgap of the QW,

$E_{g,b}$  = transitions at the upper cutoff at the bandgap of the barrier.

The more important nonradiative contributions to the current come from (1) thermal leakage of the carriers over the confining potential barriers, and (2) Auger recombination.

For interface recombination assuming identical interfaces in all of the structure for SQW, [2]:

$$J_s = 2qN_t v_s, \quad \dots(10)$$

where:

$N_t$  = QW carrier density,

$v_s$  = interface recombination velocity.

The Auger current density is given by:

$$J_A = L_z q C_A N^3, \dots(11)$$

where

$C_A$  = Auger coefficient, and the leakage current density is given by:

$$J_{lk} = e d_g N_b / t_b, \quad \dots(12)$$

where:

$N_b = 2(m_b kT / 2p \hbar^2)^{3/2}$  is the leakage carrier concentration at the barrier,

$d_g$  is the guided thickness,

$t_b$  is the lifetime for the electrons into the guiding region above the barrier potential.

**Results and Discussion:**

In this section the results obtained by using the above equations are for SQW GaAs/AlGaAs laser.

Fig.(1a, b, c, d) shows the peak modal gain versus the injected carrier density at well thickness of  $Lz = (200, 150, 100, 75) \text{ \AA}$ , respectively. The high gain sensitivity of  $g_{max}$  to changes in the number of injected electrons for different well widths, the gain is reach to threshold after ( $N=6 \times 10^{18}$ ) because the gain was calculate theoretically from (eq.5) where the effect of the intraband scattering neglected and take only TE polarization. Because of their high density of states, narrow wells could be useful when high gain values are needed.

Fig.(2) shows the relation between the value of the zero gain injection (transparency) versus the well thickness obtained from Fig.(1), from this figure the value of transparency shifts down to a lower injection current as  $Lz$  increases, these results are approximated by a linear relationship,

$g_{max} = B(N_t - N_{tr})$  [10], where  $g_{max}$  is the peak gain,  $N_{tr}$  is the carrier density at transparency,  $N_t$  is the injected carrier density,  $B$  is differential gain coefficient of the semiconductor.

Unavoidable nonradiative and leakage current components are known to contribute to the total current, leading to possibly substantial deviation from the idealization. These mechanisms for such nonideal contributions have been considered,

(1) Nonradiative transitions inside the QW's, which includes bulk and interface recombination via defect states in the bandgap, as well as Auger recombination; (2) carrier "leakage" over the top of the QW's into the continuum of the bulk- like states, including spillage sideways to the barrier layers, and, eventually, to the cladding layers, possibly involving recombination from the higher lying indirect conduction band valleys (L and X).

Fig.(3) is a 3-D plot of the interface recombination current versus the QW carrier density and the interface recombination velocity, the figure clearly demonstrates the severity of interface recombination, particularly at low  $N$  values. It needs to be stressed that interface recombination is the only nonideal contribution to the current that affects primarily the region of lower injection

carrier density, which is the preferred operating region of QW lasers. Therefore, technological attention to the quality of the interfaces during epitaxial growth is of utmost importance.

Fig.(4) is a 3-D plot of the Auger recombination current density, the QW carrier density, and the thickness of the well. In the Auger effect, the energy released by a recombining electron is absorbed by another electron (or hole), which then dissipates the energy by the emission of phonons, which becomes proportional to  $N^3$ . It is apparent that Auger recombination is largely negligible in GaAs except for high injection densities. Its contribution is below 20% for  $N < 5 \times 10^{18} \text{ cm}^{-3}$ .

Fig.(5) is a 3-D plot of the QW leakage current density with the QW injection carrier density and carrier lifetime, with QW thickness  $L_z = 75 \text{ \AA}$ . The carrier leakage out the QWs within the guiding region can be estimated from the potential steps formed at the QW hetero-interfaces and the positions of the quasi-Fermi levels. Since the carrier diffusion lengths are generally large compared with the typical thickness of the overall guiding region in the structure. It seems to be that the leakage component behaves very similarly to the Auger component of being negligible except at a high injection. There, its contribution reaches values somewhat larger than the Auger current when  $N > 6.2 \times 10^{18} \text{ cm}^{-3}$ . The carrier leakage out of the QW is very temperature sensitive, and this may lead to a substantial contribution to the temperature dependence of threshold current in a QW laser.

Fig.(6) shows the relation between the radiative current density for different QW thickness ( $L_z = 75 \text{ \AA}$ ,

$100 \text{ \AA}$ ,  $150 \text{ \AA}$ ,  $200 \text{ \AA}$ ) was drawn against the injected carrier density, to obtain the spectral gain maximum versus current density, the radiative component of the current is calculated by integration of the spontaneous emission, at higher injection levels the situation becomes more favorable, because the radiative current increases more rapidly due to bimolecular nature roughly proportional to  $N_i$ .

It can be seen that increasing the carrier density for  $L_z = 200 \text{ \AA}$  will result in a decrease of the value of the injected carrier density, from these four figures we can see that the optimum value for QW width to achieve the lower threshold current density  $J_{th} = 481.5 \text{ A/cm}^2$  at the same injected carrier density is  $L_z = 100 \text{ \AA}$ .

### Conclusions

We have studied the dynamical behavior of SQW GaAs/AlGaAs laser theoretically. By this study the peak modal gain and the radiative and nonradiative current densities for SQW GaAs/AlGaAs laser were investigated with varying the well widths  $L_z = (200, 150, 100, \text{ and } 75) \text{ \AA}$ , at a bandgap discontinuity of  $\Delta E_c$  of  $0.1 \text{ eV}$ , it was found that the highest value of the peak modal gain  $g_{max} = 400 \text{ cm}^{-1}$  is achieved at  $L_z = 75 \text{ \AA}$ , and the lower value to achieve transparency  $N_t = 0.5 \times 10^{18} \text{ cm}^{-3}$  at  $L_z = 200 \text{ \AA}$ .

In this work, it was found that the optimum value for QW width to achieve the lower threshold current density  $J_{th} = 481.5 \text{ A/cm}^2$  at the same injected carrier density is  $L_z = 100 \text{ \AA}$ .

### References

- [1] Peter S. Zory, "Quantum Well Lasers", 1993, Academic Press, Inc.
- [2] Dr.W.Koechner, "Solid-state laser engineering", Sixth Edition, Springer Series, 2006.

- 
- [3] D. Kouznetsov, et.al," Surface loss limit of the power scaling of a thin -disk laser", J. Opt.Soc.Am.B23, No.6, 2006.
- [4] S. R. Chinn, P.S.Zory, A.R. Reisinger, "A Model for GRIN-SCH-SQW Diode Laser", IEEE Journal of Quantum Electronics, Vol. 24, No.11, pp.2191-2214, November 1988.
- [5] Ralf Wilhelm, et.al., "Power scaling of end - pumped solid-state rod lasers by Longitudinal dopant concentration gradient" IEEE J. QE.Vol.44, No.1, 2008.
- [6] O.Svelto, "Principles of Lasers", Plenum Press, New York, 1998.
- [7] D. Kouznetsov, et.al," Scaling laws of a thin disk laser" J.Opt.Soc.Am.B22, No.4, 2006.
- [8] J. Hader,J.V. Moloney,S.W.Khoch, "Temperature Dependence of Radiative and Auger Loss in Quantum Wells", IEEE Journal of Quantum Electronics, Vol.44, No.2, February, 2008.
- [9] R. Muller,"A Theoretical Study of the Dynamical Behavior of Single Quantum- Well Semiconductor Lasers",Vol.91,Optics Communication, pp.453-464, 1992.
- [10] A. Yariv,"Optical Communication in Modern Communication", Oxford university Press, 1997.

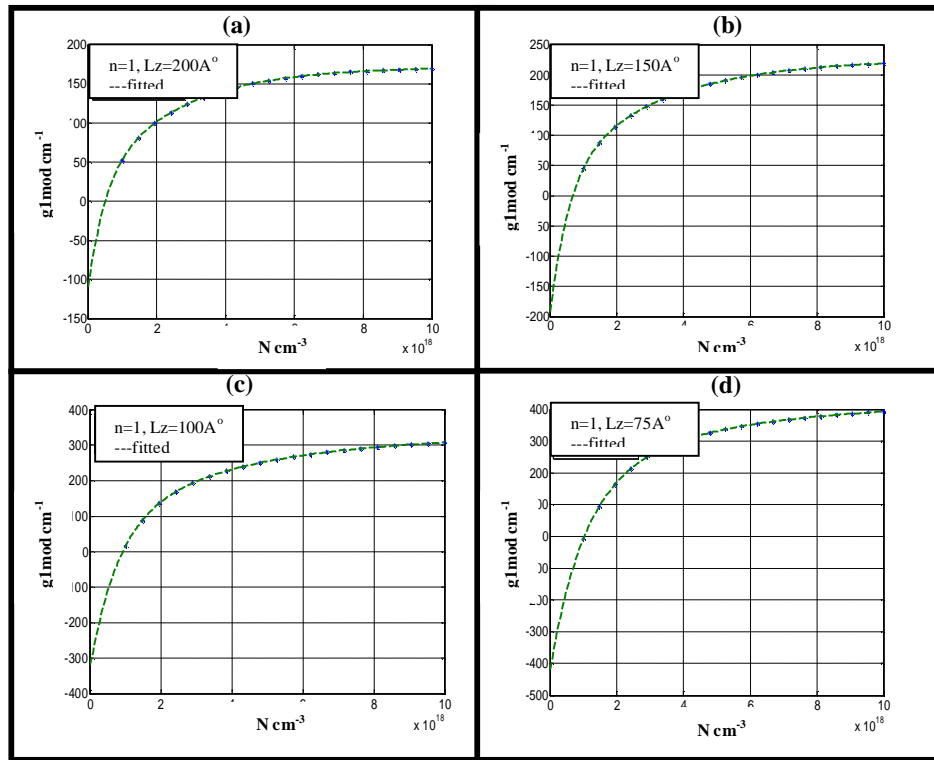


Figure (1) Peak modal gain versus the injected carrier density at, (a)  $L_z=200 \text{ \AA}$ , (b)  $L_z=150 \text{ \AA}$ , (c)  $L_z=100 \text{ \AA}$ , (d)  $L_z=75 \text{ \AA}$ .

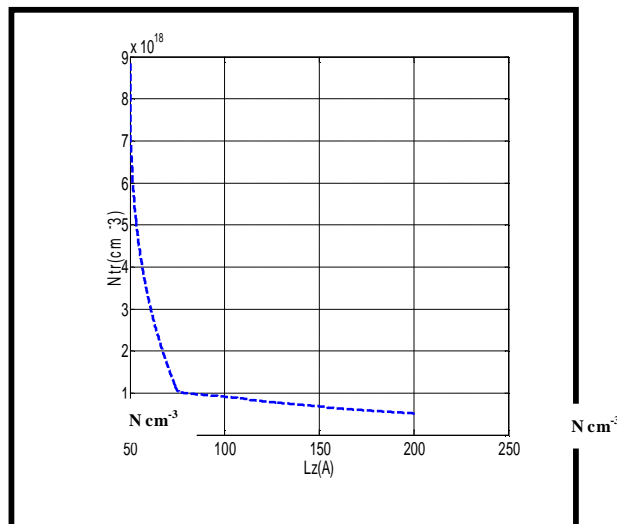


Figure (2) plot of the transparency carrier density versus the well thickness

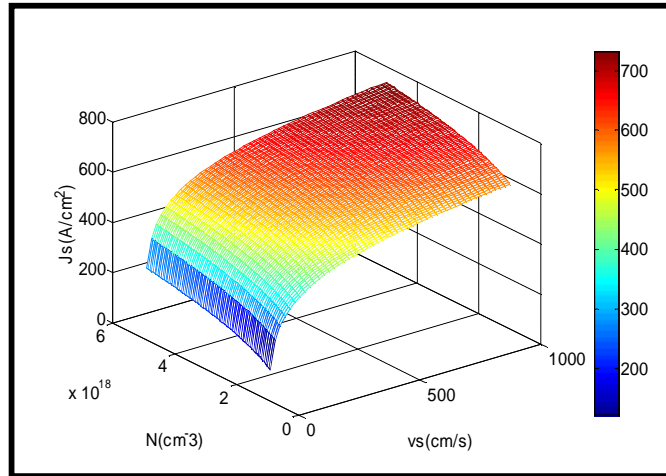


Figure (3) 3-D plot of the interface recombination current density ( $\log J_s$ ) versus the recombination velocities and QW injection carrier density  $N$ .

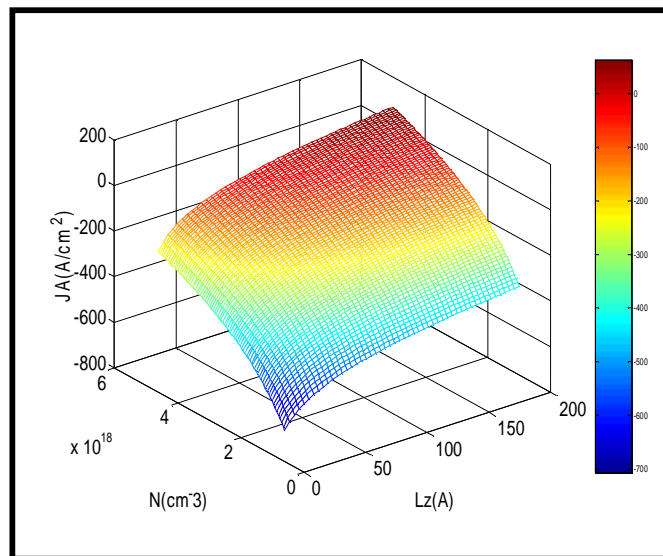


Figure (4) 3-D plot of the Auger recombination current density ( $\log J_A$ ) versus QW injection carrier density, and the QW thickness.



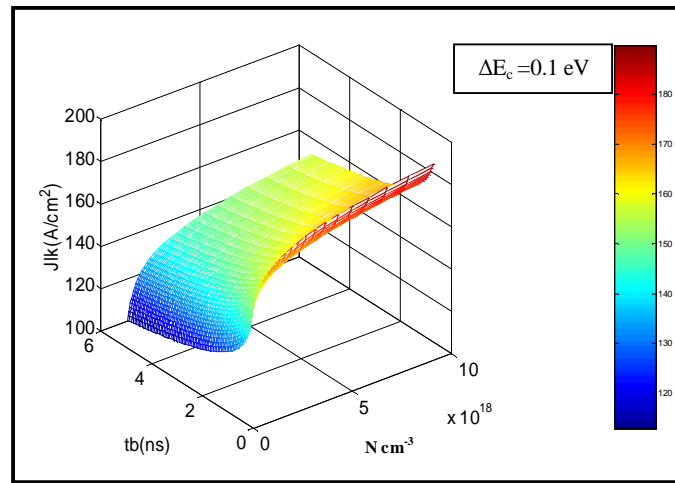


Figure (5) 3-D plot of the QW leakage current density versus QW injection carrier density and carrier lifetime, with  $L_z=75 \text{ \AA}$

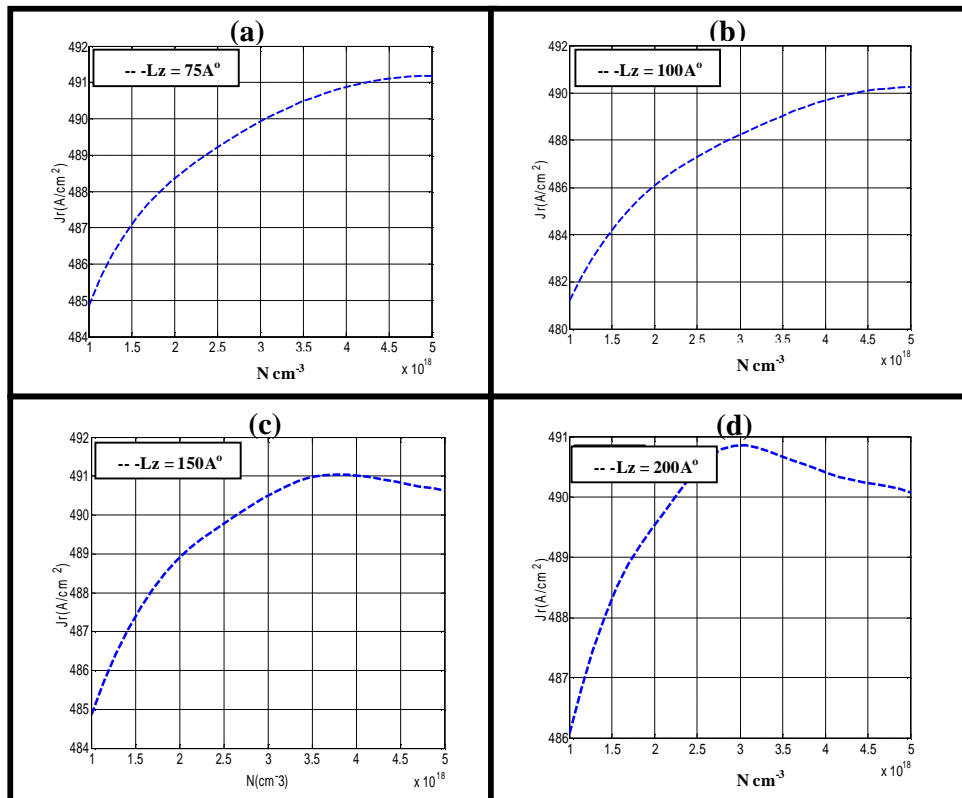


Figure (6) plot of the radiative current density ( $\log J_r$ ) versus the injected carrier density at, (a)  $L_z=75 \text{ \AA}$ , (b)  $L_z=100 \text{ \AA}$ , (c)  $L_z=150 \text{ \AA}$ , (d)  $L_z=200 \text{ \AA}$ .